Solid Earth Discuss., 6, 1423–1449, 2014
www.solid-earth-discuss.net/6/1423/2014/
doi:10.5194/sed-6-1423-2014

Solid Earth Discussions
Open Access

Active layer thermal monitoring at Fildes Peninsula, King George Island, Maritime Antarctica

R. F. M. Michel[1], C. E. G. R. Schaefer[2], F. N. B. Simas[2], Francelino M. R.[2], E. I. Fernandes-Filho[2], G. B. Lyra[3], and J. G. Bockheim[4]

[1]Universidade Estadual de Santa Cruz, Ilhéus, Brazil
[2]Universidade Federal de Viçosa, Viçosa, Brazil
[3]Universidade Federal Rural do Rio de Janeiro, Seropedica, Brazil
[4]University of Wisconsin, Madison, USA

Received: 31 March 2014 – Accepted: 7 April 2014 – Published: 1 July 2014

Correspondence to: R. F. M. Michel (roberto@michel.com)

Published by Copernicus Publications on behalf of the European Geosciences Union.

Abstract

International attention to the climate change phenomena has grown in the last decade; the active layer and permafrost are of great importance in understanding processes and future trends due to their role in energy flux regulation. The objective of the this paper is to present active layer temperature data for one CALM-S site located at Fildes Peninsula, King George Island, Maritime Antarctica over an fifth seven month period (2008–2012). The monitoring site was installed during the summer of 2008 and consists of thermistors (accuracy of ±0.2 °C), arranged vertically with probes at different depths, recording data at hourly intervals in a high capacity data logger. A series of statistical analysis were performed to describe the soil temperature time series, including a linear fit in order to identify global trend and a series of autoregressive integrated moving average (ARIMA) models were tested in order to define the best fit for the data. The controls of weather on the thermal regime of the active layer have been identified, providing insights about the influence of climate chance over the permafrost. The active layer thermal regime in the studied period was typical of periglacial environment, with extreme variation at the surface during summer resulting in frequent freeze and thaw cycles. The active layer thickness (ALT) over the studied period showed variability related to different annual weather conditions, reaching a maximum of 117.5 cm in 2009. The ARIMA model was considered appropriate to treat the dataset, enabling more conclusive analysis and predictions when longer data sets are available. Despite the variability when comparing temperature readings and active layer thickness over the studied period, no warming trend was detected.

1 Introduction

International attention on the climate change phenomena has grown in the last decade, intense modeling of climate scenarios were carried out by scientific investigations searching the sources and trends of these changes (Mora et. al, 2013; IPCC, 2012;

Moss et. al., 2010). The cryosphere and its energy flux became the focus of many investigations, being recognized as a key component of climate for the understanding of actual (climate variability) and future trends (Ledley, 2012; Flanner et. al., 2011; van den Broeke et. al., 2008). The active layer and permafrost, part of the terrestrial cryosphere, are of great importance due to their role in energy flux regulation and sensitivity to climate change (Kane et al., 2001; Smith and Brown, 2009). Compared with other regions of the globe, our understanding of Antarctic permafrost is poor, especially in relation to its thermal state and evolution, its physical properties, links to pedogenesis, hydrology, geomorphic dynamics and response to atmosphere, and thus, the variability and global climate change (Bockheim, 1995; Bockheim et al., 2008). An understanding of the distribution and properties of Antarctic permafrost is essential for the cryospheric sciences, but also for life sciences, since it will be a major control on ecosystem modification following climate induced changes and variability (Vieira et. al., 2009). The scientific interest in King George Island has grown in the last few years due to the intensity of climate change effects, in consequence of which permafrost degradation is observed (Beyer et al., 1999).

The objective of the this paper is to present active layer temperature data for one CALM-S site located at Fildes Peninsula, King George Island, Maritime Antarctica over a fifth seven month period (2008–2012).

2 Material and methods

2.1 Studied site

The archipelago of the South Shetland Islands, extending more than 400 km from southwest to northeast, lies near the northern tip of the Antarctic Peninsula. The archipelago is separated from the Antarctic Peninsula by the Bransfield Strait and from South America by Drake Passage. King George Island is the largest in the archipelago and Fildes Peninsula is at its southwestern end (Fig. 1). This peninsula is about 10 km long and 2–4 km wide. It is washed on three sides by the waters of Drake Passage, Fildes Strait, and Maxwell Bay. Most of the Fildes Peninsula is free of ice; glaciers cover only the extreme northeastern part (Simonov, 1977).

The region experiences a sub-antarctic maritime climate, according to the Köppen climate classification, the South Shetland Islands have an ET climate, South Hemispheric Polar Oceanic (Köppen, 1936), characterized by mean annual air temperatures of –2.2 °C (data from 2000 through 2012, Marsh met station – 62°11′27″ S, 58°59′12″ W, and 10 m of altitude) and mean summer air temperatures above 0 °C up to four months (Rakusa-Suszczewski et al., 1993; Wen et al., 1994); precipitation ranges between 350 and 500 mm per year, with rainfall occurring in the summer period (Øvstedal and Smith, 2001). Ferron et al. (2004) found great climate variability when analyzing data from 1947 to 1995 and identified cycles of 5.3 years of colder conditions followed by 9.6 years of warmer conditions.

3 Methods

The active layer monitoring site (– 62°12′12″ S, 58°57′37″ W, and 60 m of altitude) was installed (10.5 cm (F1), 32.5 cm (F2), 67.5 cm (F3), 83.5 cm (F4)) in the summer of 2008, and consist of thermistors (accuracy ±0.2 °C) (model 107 Temperature Probe, Campbell Scientific Inc, Utah, USA) arranged in a vertical array at different depths down to the permafrost table, the site was selected during soil survey and represents most of Turbic Cryosols occurring at the peninsula. All probes were connected to a data logger (model CR 1000, Campbell Scientific Inc, Utah, USA) recording data at hourly intervals from 1 March 2008 until 30 November 2012.

The characteristics of the monitored site and the exact depth of the probes are presented in Tables 1 and 2, the depth of the probes was established respecting pedological differentiation of horizons. Air temperature was obtained from Marsh automatic met station, located at Teniente Marsh Air Port.

SED
6, 1423–1449, 2014

We calculated the thawing days (days in which all hourly soil temperature measurements are positive and at least one reading is warmer than +0.5 °C), freezing days, (days in which all hourly soil temperature measurements are negative and at least one reading is colder than −0.5 °C); number of isothermal days (days in which all the hourly measurements range only between ±0.5 °C) and the number of freeze–thaw days (days in which there are both negative and positive temperatures with at least one value greater than ±0.5 °C); the thawing degree days (TDD, obtained by the cumulative sum of the mean daily temperatures above 0 °C); the freezing degree days (FDD, obtained by the cumulative sum of the mean daily temperatures below 0 °C); according Guglielmin et al. (2008). The active layer thickness (ALT) was calculated as the 0 °C depth by extrapolating the thermal gradient from the two deepest temperature measurements (Guglielmin, 2006).

The apparent thermal diffusivity (ATD) was estimated for different seasons from the equation of McGaw et al. (1978):

$$\alpha = [\Delta Z^2/2\Delta t] \times \left[\left(T_i^{j+1} - T_i^{j-1}\right) / \left(T j i^{-1} - 2T_j^i + T_j^{i+1}\right)\right] \quad (1)$$

where α = apparent thermal diffusivity ($m^2\,s^{-1}$), Δt = time increments (s), ΔZ = space increments (m), T = temperature, j = temporal position and i = depth position. Nelson et al. (1985), Outcalt and Hinkel, (1989), Hinkel et al. (1990, 2001) have used this estimative to assess the resistance to energy flux in the profile. Hourly estimations were made for intermediate depths of both profiles, and mean values were calculated and plotted for each day.

A series of statistical analysis were performed to describe the soil temperature time series. The Box–Pierce test and Augmented Dickey–Fuller tests where performed to confirm the stationarity and independent distribution of the time series (data not shown). Plotting it's histogram (frequency distribution of temperature readings) and first difference (the difference between consecutive hourly temperature readings) were performed and the time series was decomposed into it's seasonal and trend components by locally weighted smoothing (Loess) using a window of 25. A linear fit was applied

SED
6, 1423–1449, 2014

to the time series in order to identify global trend and finally a series of autoregressive integrated moving average (ARIMA) models were tested until satisfactory results were found. In order to define the best fit for the data we first examined the ACF and PACF plots to determine the appropriate model, then a series of combinations were tested; Standardized Residuals, Autocorrelation plot, Ljung-Box statistics and Akaike's Information Criterion (AICc) (Burnham and Anderson, 2002) where the major parameters used to judge suitability of the model. Considering the seasonal nature of the data, after the best models were selected a seasonal component was added.

For a time series of data x_t, where t = time and x = real number, soil temperature in the present case, then a ARMA model:

$$\left(1-\sum_{i=1}^{p'}\phi_i L^i\right)x_t=\left(1+\sum_{i=1}^{q}\theta_i L^i\right)\varepsilon_t \quad (2)$$

where, p' = autoregressive terms, q = moving-average terms, L = lag operator, ϕ = autoregressive parameter, θ = moving average parameter, ε = error and i = ith term. The error are assumed to be independent, identically distributed variables sampled from a normal distribution with zero mean and one standard deviation [0,1].

Whereas the term $\left(1-\sum_{i=1}^{p'}\phi_i L^i\right)$ has a unitary root of multiplicity d. Then it can be rewritten as:

$$\left(1-\sum_{i=1}^{p'}\phi_i L^i\right)=\left(1-\sum_{i=1}^{p'-q}\phi_i L^i\right)(1-L)^d \quad (3)$$

An ARIMA (p, d, q) model expresses this polynomial factorization property with $p=p'-d$, and is express by:

$$\left(1-\sum_{i=1}^{p}\phi_i L^i\right)(1-L)^{\mathrm{d}}x_t=\left(1+\sum_{i=1}^{q}\theta_i L^i\right)\varepsilon_t \quad (4)$$

SED
6, 1423–1449, 2014

and thus can be thought as a particular case of an ARMA($p+d,q$) process having the autoregressive polynomial with d unit roots.

4 Results and discussion

4.1 Results and discussion

Interannual variability of the active layer temperature shows parallel behavior despite contrasts between different years, daily temperatures records are presented in Fig. 2. The temperature at 10.5 cm reaches a maximum daily average (4.06 °C ± 0.46) in early January, reaching a minimum (−8.03 °C ± 1.36) between late July and early August. At 83.5 cm maximum temperature (0.30 °C ± 0.24) occurs in late March and the minimum reading (−4.06 °C ± 0.98) was recorded around mid August. Disparities can be noticed when comparing the different years; 2008 had a mild winter (21 freezing days and −0,88 freezing degree days at 83.5 cm in July) contrasted by a severe winter in 2011 (31 freezing days and −80,00 freezing degree days at 83.5 cm in July), the summer of 2009 was considerably warmer (31 thawing days and 64.77 thawing degree days at 10.5 cm in January) compared to the summer of 2010 (17 thawing days and 21,15 thawing degree days at 10.5 cm in January).

Daily Air temperature at Fildes Peninsula over the studied period averaged −2.3 °C (±4.1), reaching a maximum and a minimum of 5.75 °C and −21.20 °C, in early January and late June, respectively. The difference between maximum and minimum daily averages was greater for 2009 and 2011, in this years more extreme minimum temperatures were recorded (−17.4 °C for 2009 and −18.6 °C for 2011). The freezing season started in late May and the thawing season in mid December with small variability between the years. Soil temperature averaged −1.2 °C (avg. max 2.1 °C and avg. min −7.3 °C) considering all layers, maximum soil temperature for the upper most layer (F1) considering hourly measurements was 8.7 °C and minimum −9.8 °C and 0.5 °C and −5.4 °C at the bottom most layer (F4).

SED
6, 1423–1449, 2014

ALT was estimated for every season, results summarized in Table 1 (2008 and 2012 being incomplete), maximum ALT ranged between 89.0 cm and 105.8 cm, mean 101.0 cm; the totality of the active layer froze during winter every year over the studied period. During 2010 curious phenomena occurred, temperatures at F3 remained negative the whole year, reaching values above zero at the bottom most layer (F4), in this year ATL was estimated slightly below the deepest probe, this is probably due to the accumulation of water over the permafrost table.

The grouping of days in Freezing, Thawing, Isothermal and Freeze Thaw offers a quick parameter for comparing different periods (Fig. 3). Most of Thawing Days occur between January and March, more frequently for the upper most layers, only eight days were recorded for F4 in March 2009. Freeze Days are concentrated between April and November, these are more evenly distributed in depth although F1 and F2 where frozen for longer periods in 2008, 2011 and 2012. Isothermal and Freeze Thaw Days occur between December and May, Isothermal periods are long for F3 and F4 which show a strong zero curtain effect (buffered temperature change due to freezing and thawing of soil moisture); Freeze Thaw Days are more common in F1, the site experiences frequent freeze thaw cycles in surface, specially during summer; great temperature changes in depth, specially on the −0.5 °C to 0.5 °C zone are rare, only one day was recorded in 2011 for F4.

The cumulative sum of the daily averages reached an maximum in 2009 and a minimum in 2011 for all layers, values varied greatly over the years, December and January being the hottest months and June always the coldest (Fig. 4). Over all the 57 months the TDD were 901.7 °C day (F1), 448.9 °C day (F2), 95.6 °C day (F3) and 64.0 °C day (F4) and the FDD were −3229.0 °C day (F1), −2623.1 °C day (F2), −2433.3 °C day (F3), −2040.8 °C day (F4). Contrast between different years was significant, in 2011 FDD accumulated −819 °C day in surface and −516 °C day at F4; in contrast 2011 accumulated −527 in surface and −382 at F4. There is a clear preponderance of negative soil temperatures in the studied profile, despite the percolation of liquid water and above freeze temperatures during summer, positive temperatures are mild in the soil profile.

ATD was calculated for F3 and F4 considering hourly readings and then average for the climatic seasons, results are shown in Table 3. Thermal diffusivity can experience considerable seasonal variations when thawing and freezing processes occur (Hinkel, 1997). The ability of the profile in transmitting energy varies during the year mostly due to water content, moist on one hand enhances energy flux through percolation and on the other hand absorbs and emits energy on freezing and thawing processes. Average ATD for the 57 months was $4.2 \times 10^{-5}\,m^2\,s^{-1}$ (F2) and $1.1 \times 10^{-5}\,m^2\,s^{-1}$ (F3), values are consistent with other findings from wet soil profiles of Maritime Antarctica, De Pablo et al. (2013) found values of $4.7 \pm 0.7 \times 10^{-7}\,m^2\,s^{-1}$ and $5.3 \pm 1.8 \times 10^{-7}\,m^2\,s^{-1}$ for the summer period in a profile from Byers Peninsula, Livingstone Island. ATD calculated for F2 has tendency of smaller values for winter being negative for fall and winter of 2009, when abnormally cold temperatures occurred and the thaw season was reduced at 32.5 cm. Values for F3 are consistently smaller due to its proximity to the permafrost table, negative values are more common, occurring in winter and spring of 2008, fall and winter of 2009 and winter of 2010 and 2011. This behavior indicates temperature buffering capacity, negative ATD values suggests that nonconductive effects oppose and overwhelm the conductive trend (Outcalt and Hinkel, 1989).

Histograms for the studied layers show a predominance of temperatures around zero, F3 expressed the largest frequency in this region; the greatest amplitude is found for F1 (15 °C) (Fig. 5). The plot of first differences of the hourly measurements give us an idea of periods with great temperature oscillation, most of the strong variations are associated with summer for F1 and F2, being evenly distributed for F3 and very limited for F4 (Fig. 5). The decomposition of the time series reveals great seasonal component associated with summer for F1 and F2, most of the noise is also concentrated in the warmer months; F3 behaves more erratically and at F4 the seasonal effect is shifted ahead, while noise is reduced (Fig. 6). Linear regression was performed on hourly readings in order to have an estimation of over all trend, the slope of the line is slightly negative for all layers and intercept is always negative (Fig. 7).

Although the studied period is limited to 57 months and any forecast is not suitable, an ARIMA model was tested to each layer in order to evaluate which model better fits the data. Autocorrelation and partial autocorrelation plots were estimated as a guide for the selection of the ARIMA parameters. The plots (Fig. 8) shows strong correlation with data from the previous month, this correlation is smaller for the subsequent period and after the forth month it starts to show increasing negative correlation, reaching a maximum at the seventh month; after three years significant correlation can still be seen. Partial autocorrelations expresses a "cleaner" picture of serial dependencies for individual lags, the plot shows a strong correlation for the previous month which is negative for the subsequent period and not significant after the fifth lag. The best ARIMA model that fitted the monthly averages included seasonal components (P, D, Q); p, d and q factors. Its seasonal components were always small or null, as indicated by the partial autocorrelations. The best model for F1 and F3 included one autoregressive parameter, one seasonal autoregressive parameter and one seasonal differentiating parameter (Table 4), the best model for F2 included only seasonal parameters, one seasonal autoregressive parameter and one seasonal differentiating parameter whereas the best fit for F4 included one autoregressive parameter, two moving average parameters and two seasonal autoregressive parameters. The diagnostics of the models (Fig. 9) where satisfactory, the standardized residuals did not shows clusters of volatility, no significant auto correlation was found between the residuals and the ρ values for the Ljung–Box statistics are all large, indicating that the residuals are pattern less.

5 Conclusions

Monitoring of the CALM-S site on Fildes Peninsula provided data on the thermal dynamics and frost conditions in a densely vegetated Maritime Antarctic site. The controls of weather on the thermal regime of the active layer have been identified, providing information on how climate changes influence active layer and permafrost, as follows:

- The active layer thermal regime in the studied period was typical of periglacial environments, with extreme variation in surface during summer resulting in frequent freeze and thaw cycles.
- The ALT over the studied period shows a degree of variability related to different annual weather conditions, reaching a maximum of 117.5 cm in 2009.
- The calculated ATD apparent thermal diffusivity suggests strong influence of water content and snowpack to the soil thermal regime.
- The ARIMA model is an important tool for more conclusive analysis and predictions when longer data sets are available.
- Despite the variability when comparing temperature readings and active layer thickness over the studied period no trend can be identified.

Acknowledgements. This study was supported technically and logistically by the Brazilian Navy, MMA, UFV and FEAM-MG; grants received from CNPq. We also thank the Chilean Antarctic Institute (INACH) for technical and logistical support during field activities. This is a contribution of the Terrantar laboratory, part of the Brazilian National Institute of Cryospheric Science and Technology.

References

Beyer, L., Bockheim, J. G., Campbell, I. B., and Claridge, G. G. C.: Genesis, properties and sensitivity of Antarctic Gelisols, Antarct. Sci., 11, 387–398, 1999.

Bockheim, J. G.: Permafrost distribution in the southern circumpolar region and its relation to the environment: A review and recommendations for further research, Permafrost Periglac. Process., 6, 27–45, 1995.

SED

6, 1423–1449, 2014

Bockheim, J. G. and Mcleod, M.: Soil distribution in the McMurdo Dry Valleys, Antarctica, Geoderma, 144, 43–49, 2008.
Burnham, K. P. and Anderson, D. R.: Model selection and multimodel inference: a practical information-theoretic approach, Springer, New York, 2 pp., 2002.
De Pablo, M. A., Blanco, J. J., Molina, A., Ramos, M., Quesada, A., and Vieira, G.: Interannual active layer variability at the Limnopolar Lake CALM site, Byers Peninsula, Livingston Island, Antarctica, Antarct. Sci., 25, 167–180, doi:10.1017/S0954102012000818, 2013.
Ferron, F. A., Simões, J. C., Aquino, F. E., and Setzer, A. W.: Air temperature time series for King George Island, Antarctica, Pesquisa Antártica Brasileira, 4, 155–169, 2004.
Flanner, M. G., Shell, K. M., Barlage, M., Perovich, D. K., and Tschudi, M. A.: Radiative forcing and albedo feedback from the Northern Hemisphere cryosphere between 1979 and 2008, Nat. Geosci., 4, 151–155, doi:10.1038/ngeo1062, 2011.
Hinkel, K. M.: Estimating seasonal values of thermal diffusivity in thawed and frozen soils using temperature time series, Cold Reg. Sci. Technol., 26, 1–15, 1997.
Hinkel, K. M., Outcalt, S. I., and Nelson, F. E.: Temperature variation and apparent thermal diffusivity in the refreezing active layer, Toolik Lake, Alaska, Permafrost Periglac., 14, 265–274, 1990.
Hinkel, K. M., Paetzold, F., Nelson, F. E., and Bockheim, J. G.: Patterns of soil temperature and moisture in the active layer and upper permafrost at Barrow, Alaska: 1993–1999, Global Planet. Change, 29–3, 293–309, 2001.
Guglielmin, M.: Ground surface temperature (GST), active layer, and permafrost monitoring in continental Antarctica, Permafrost Periglac., 17, 133–143, 2006.
Guglielmin, M., Evans, C. J. E., and Cannone, N.: Active layer thermal regime under different vegetation conditions in permafrost areas, a case study at Signy Island (Maritime Antarctica), Geoderma, 144, 73–85, 2008.
IPCC: Managing the Risks of Extreme Events and Disasters to Advance limate Change Adaptation, a Special Report of Working Groups I and II of the Intergovernmental Panel on Climate Change, edited by: Field, C. B., Barros, V., Stocker, T. F., Qin, D., Dokken, D. J., Ebi, K. L., Mastrandrea, M. D., Mach, K. J., Plattner, G.-K., Allen, S. K., Tignor, M., and Midgley, P. M., Cambridge University Press, Cambridge, UK, and New York, NY, USA, 582 pp., 2012.
Kane, D. L., Hinkel, K. M., Goering, D. J., Hinzman, L. D., and Outcalt, S. I.: Non-conductive heat transfer associated with frozen soils, Global Planet. Change, 29, 275–292, doi:10.1016/S0921-8181(01)00095-9, 2001.

Ledley, T. S.: Sea ice: multiyear cycles and white ice, J. Geophys. Res.-Atmos., 90, 2156–2202, 1985.
Mcgaw, R. W., Outcalt, S. I., and Ng, E.: Thermal properties and regime of wet tundra soils at Barrow, Alaska, in: Third International Conference on Permafrost, National Research Council of Canada, 1978, Ottawa, Canada, 47–53, 1978.
Mora, C., Frazier, A. G., Longman, R. J., Dacks, R. S., Walton, M. M., Tong, E. J., Sanchez, J. J., Kaiser, L. R., Stender, Y. O., Anderson, J. M., Ambrosino, C. M., Fernandez-Silva, I., Giuseffi, L. M., and Giambelluca, T. W.: The projected timing of climate departure from recent variability, Nature, 502, 183–187, 2013.
Moss, R. H., Edmonds, J. A., Hibbard, K. A., Manning, M. R., Rose, S. K., van Vuuren, D. P., Carter, T. R., Emori, S., Kainuma, M., Kram, T., Meehl, G. A., Mitchell, J. F., Nakicenovic, N., Riahi, K., Smith, S. J., Stouffer, R. J., Thomson, A. M., Weyant, J. P., and Wilbanks, T. J.: The next generation of scenarios for climate change research and assessment, Nature, 463, 747–56, 2010.
Nelson, F. E., Outcalt, S. I., Goodwin, C. W., and Hinkel, K. M.: Diurnal thermal regime in a peat-covered palsa, Toolik Lake, Alaska, Arctic, 38, 310–315, 1985.
Outcalt, S. I. and Hinkel, K. M.: Night frost modulation of near-surface soil–water ion concentration and thermal fields, Phys. Geogr., 10, 336–346, 1989.
Øvstedal, D. O. and Lewis-Smith, R. I.: Lichens of Antarctica and South Georgia: Guide to Their Identification and Ecology, Cambridge, Cambridge University Press, 411 pp., 2001.
Rakusa-Suszczewski, S., Mietus, M., and Piasecki, J.: Weather and climate, in: The Maritime Antarctic Coastal Ecosystem of Admiralty Bay, edited by: Rakusa-Sszczewski, S., Department of Antarctic Biology, Polish Academy of Sciences, 19–25, 1993.
Simonov, M. I.: Physical-geofraphic descriptions of the Fildes Peninsula (South Shetland Islands), Polar Geografy, 1, 223–242, 1975.
Smith, S. L. and Brown, J.: T7 Permafrost: Permafrost and Seasonally Frozen Ground, Global Terrestrial Observing System, GTOS 62, Rome, 19 pp., 2009.
Vieira, G., Bockheim, J., Guglielmin, M., Balks, M., Andrey, A., Boelhouwers, J., Cannone, N., Ganzer, L., Gilchinsky, D., Goryachkin, S., López-Martínez, J., Meiklejohn, I., Raffi, R., Ramos, M., Schaefer, C., Serrano, E., Simas, F., Sletten, R., and Wagner, D.: Thermal state of Antarctic permafrost and active-layer dynamics: advances during the International Polar Year 2007–2008, Permafrost Periglac., 21, 182–197, 2010.

SED
6, 1423–1449, 2014

van den Broeke, M., Smeets, P., Ettema, J., van der Veen, C., van de Wal, R., and Oerlemans, J.: Partitioning of melt energy and meltwater fluxes in the ablation zone of the west Greenland ice sheet, The Cryosphere, 2, 179–189, doi:10.5194/tc-2-179-2008, 2008.
Wen, J., Xie, Z., Han, J., and Lluberas, A.: Climate, mass balance and glacial changes on small dome of Collins Ice Cap, King George Island, Antarctica. Antarct. Res., 5, 52–61, 1994.

SED
6, 1423–1449, 2014

Active layer thermal monitoring at Fildes Peninsula

R. F. M. Michel et al.

Table 1. General characteristics of the monitored site.

Site	Altitude/Slope/Aspect	Soil Class WRB/Soil Taxonomy	Vegetation Cover	ALT*	Thermistor depth
Fildes	65 m/3 % max./S	Turbic Cryosol (Eutric)/ Aquic Haploturbels	Mosses and Lichens (*Usnea sp.* and *Himantormia sp.*)	102.5 cm (2008); 117.5 (2009); 90.2 cm (2010); 105.8 cm (2011); 89.0 cm (2012)	10.5 cm (F1), 32.5 cm (F2), 67.5 cm (F3), 83.5 cm (F4)

* ALT – Active Layer Thickness.

SED
6, 1423–1449, 2014

Table 2. Soil texture of the studied profile.

Depth (cm)	CS[a]	FS[b]	Silt[c]	Clay[d]	Class
	$g\,kg^{-1}$				
Fildes – Turbic Haplic Cryosol (Eutric)					
AB 0–20	28	18	34	20	Loam
B 20–50	29	17	36	18	Loam
C 50–100	14	30	47	9	Loam

[a] Coarse Sand (0.2 ≤ 2 mm),
[b] Fine Sand (0.05 ≤ 0.2 mm),
[c] 0.002 ≤ 0.05 mm,
[d] < 0.002 mm.

SED
6, 1423–1449, 2014

Table 3. Average season temperatures for Air, F1, F2, F3, and F4; and ATD for F2 and F3.

Averages	Air	F1	F2	F3	F4	ATD_F2	ATD_F3
Fall_2008	−2.36	−1.12	−0.32	−0.10	0.09	1.4E-04	6.3E-05
Winter_2008	−3.54	−3.23	−2.69	−2.19	−1.64	1.0E-05	−3.4E-06
Spring_2008	−0.28	0.38	−0.38	−0.82	−0.77	1.3E-04	−8.8E-06
Summer_2009	1.64	2.55	1.55	0.37	0.11	3.5E-05	2.6E-07
Fall_2009	−2.49	−1.49	−0.48	−0.11	0.11	−1.9E-04	−1.3E-05
Winter_2009	−6.40	−4.95	−4.19	−3.52	−2.86	−9.3E-07	−4.0E-06
Spring_2009	−1.96	−1.66	−1.79	−2.02	−1.87	1.1E-05	1.1E-05
Summer_2010	0.41	1.44	0.49	−0.33	−0.27	2.3E-04	5.9E-06
Fall_2010	−2.24	−1.25	−0.62	−0.43	−0.21	1.5E-04	1.6E-05
Winter_2010	−4.09	−3.70	−3.27	−2.92	−2.45	8.4E-06	−1.0E-06
Spring_2010	−0.63	−0.38	−0.87	−1.30	−1.23	2.9E-05	2.9E-05
Summer_2011	1.63	2.22	1.34	0.21	−0.02	2.9E-05	1.9E-06
Fall_2011	−4.28	−1.75	−0.60	−0.12	0.09	8.6E-05	2.9E-05
Winter_2011	−7.91	−5.69	−4.93	−4.19	−3.51	4.8E-08	−5.9E-06
Spring_2011	−1.21	−1.14	−1.60	−2.04	−1.99	6.3E-06	1.6E-05
Summer_2012	1.35	1.86	0.94	−0.18	−0.20	4.4E-05	5.0E-05
Fall_2012	−3.91	−1.66	−0.72	−0.36	−0.09	1.0E-06	1.1E-05
Winter_2012	−5.47	−4.33	−3.88	−3.55	−3.04	6.8E-06	7.3E-07
Spring_2012	−3.14	−2.08	−2.19	−2.47	−2.33	3.4E-05	1.2E-05
AVG	−2.18	−1.18	−1.14	−1.29	−1.10	4.2E-05	1.1E-05
Standard Deviation	2.75	2.45	1.90	1.45	1.25	8.3E-05	1.9E-05

SED
6, 1423–1449, 2014

Active layer thermal monitoring at Fildes Peninsula

R. F. M. Michel et al.

Table 4. ARIMA order, coefficients sigma squared and log of likelihood for F1, F2, F3, and F4.

ARIMA	F1	F2	F3	F4
Order (seasonal)	(1,0,0) (1,1,0)	(0,0,0) (1,1,0)	(1,0,0) (1,1,0)	(1,0,2) (2,0,0)
Coefficients	ar1 0.2540 sar1 −0.5507	ar1 0.2568 sar1 −0.7355	ar1 0.3534 sar1 −0.7224	ar1 0.5030 ma1 0.2355 ma2 −0.0322 sar1 00.2536 sar2 0.6152
$Sigma^2$	2.17	0.85	0.44	0.25
log likelihood	−83.53	−64.91	−50.01	−50.88
AICc	173.65	136.41	106.6	118.06
BIC	178.49	141.25	111.44	130.07

SED
6, 1423–1449, 2014

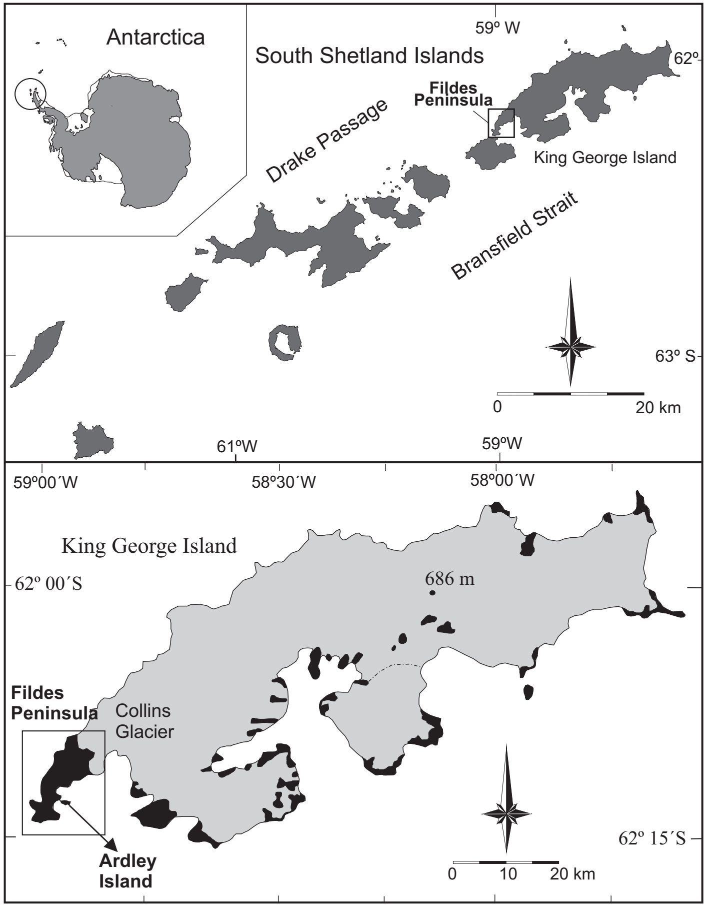

Figure 1. Location of Fildes Peninsula within Antarctica and the South Shetland Islands.

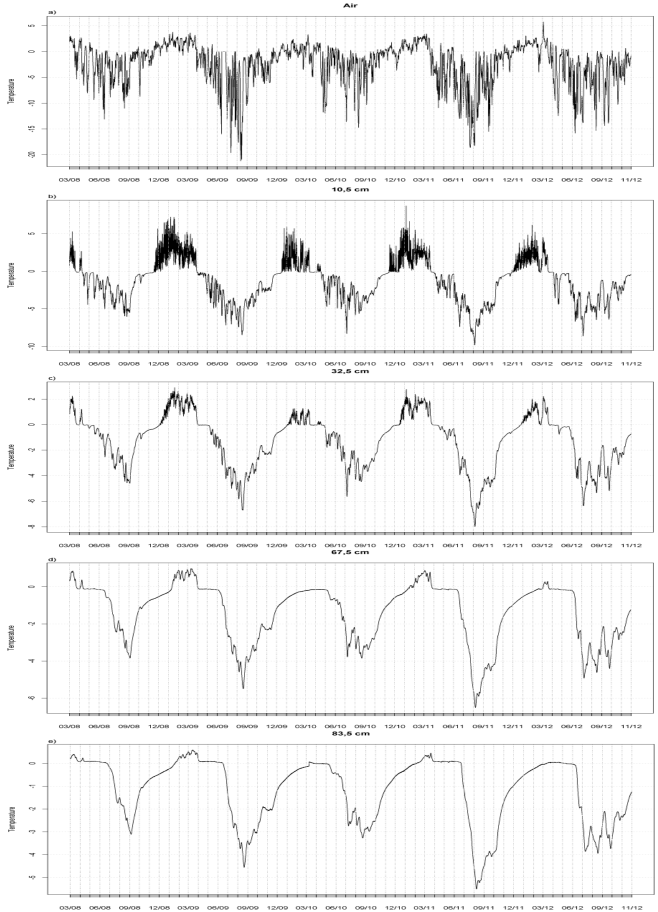

Figure 2. Daily temperatures records for Air **(a)**, F1 **(b)**, F2 **(c)**, F3 **(d)** and F4 **(e)**.

SED
6, 1423–1449, 2014

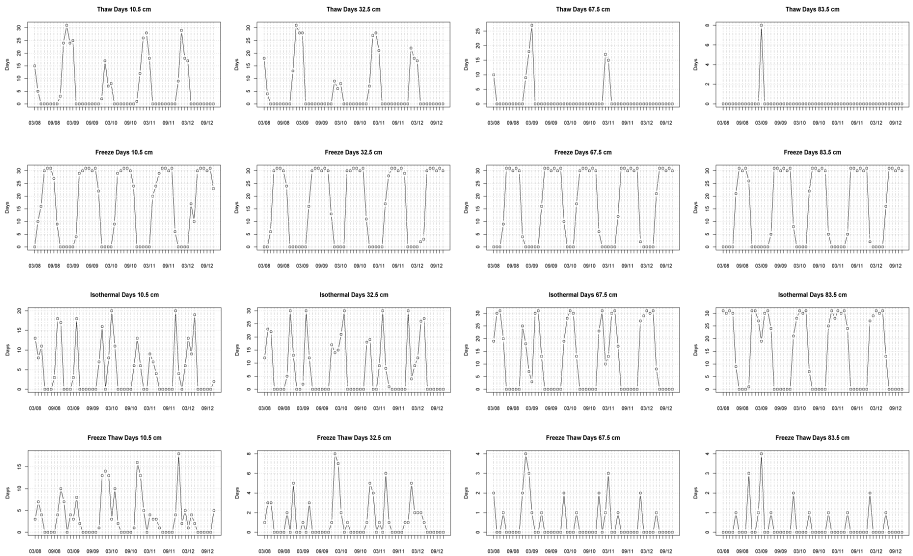

Figure 3. Thaw days, freeze days, isothermal days and freeze thaw days for F1, F2, F3 and F4.

SED
6, 1423–1449, 2014

Active layer thermal monitoring at Fildes Peninsula

R. F. M. Michel et al.

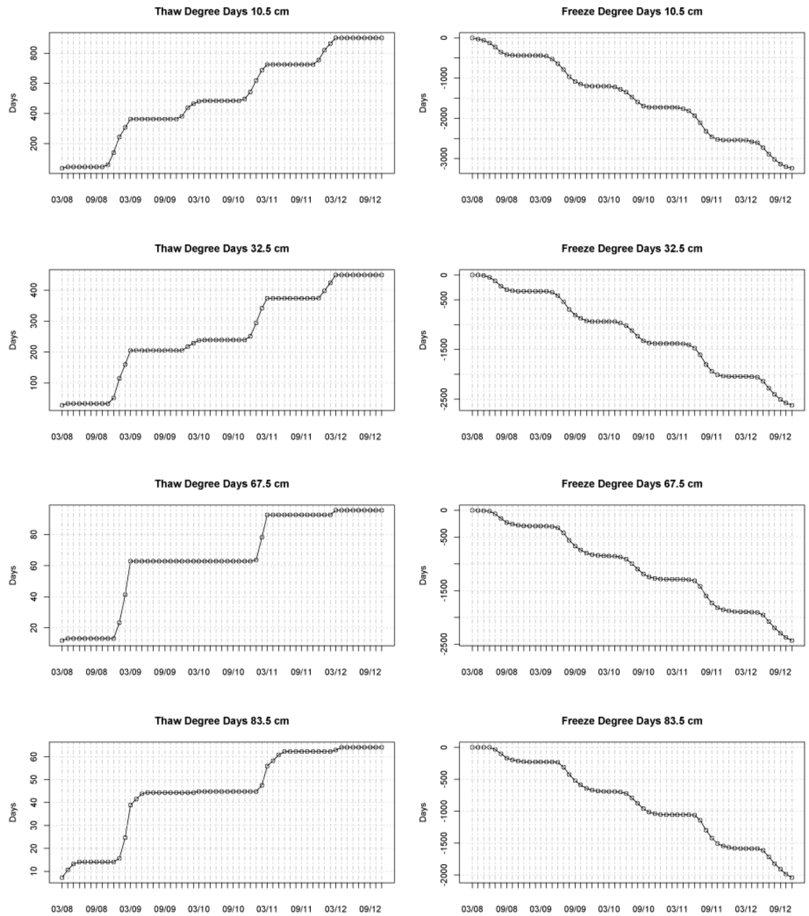

Figure 4. Thaw degree days and freeze degree days for F1, F2, F3 and F4.

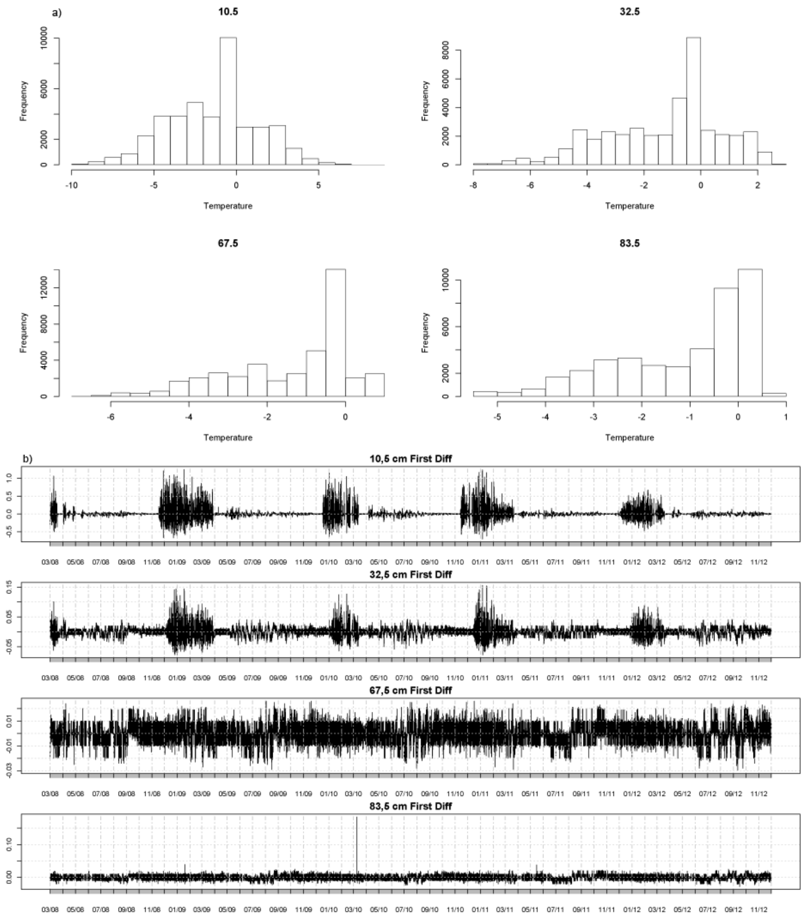

Figure 5. Histograms and first difference for F1, F2, F3 and F4.

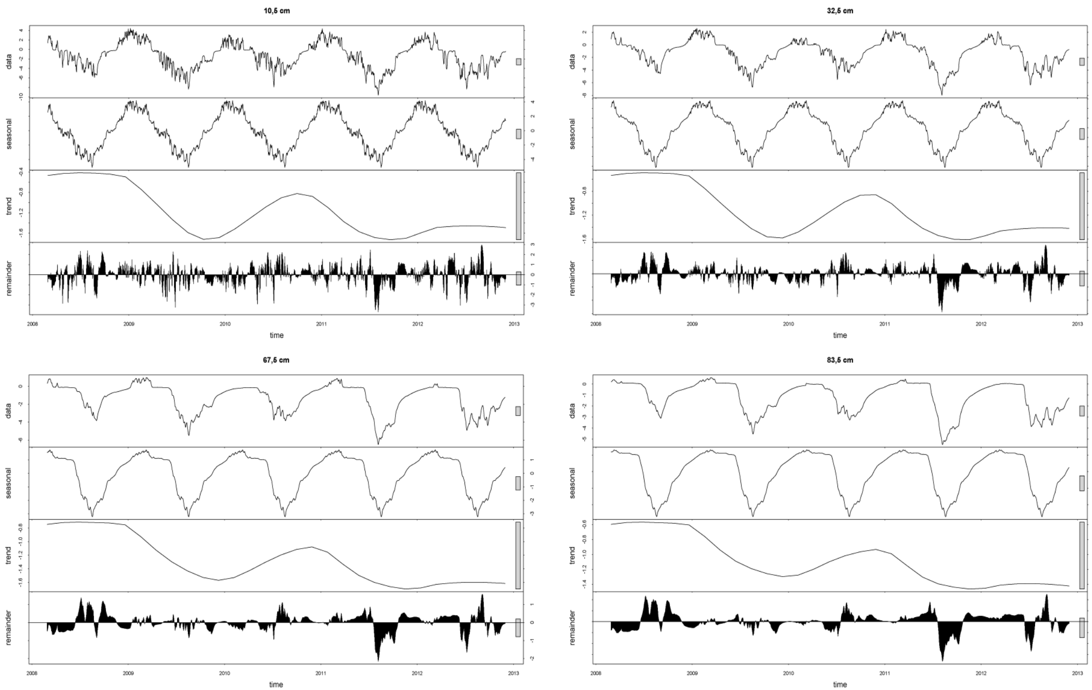

Figure 6. Loess time series decomposition for F1, F2, F3 and F4.

SED

6, 1423–1449, 2014

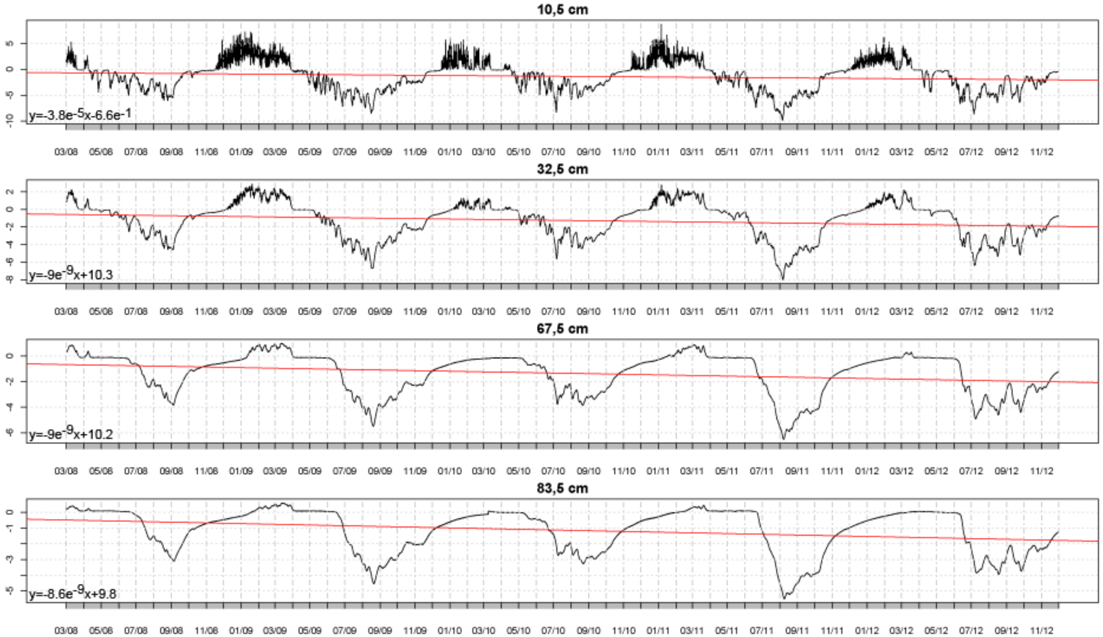

Figure 7. Linear Regression for F1, F2, F3 and F4.

SED
6, 1423–1449, 2014

Active layer thermal monitoring at Fildes Peninsula

R. F. M. Michel et al.

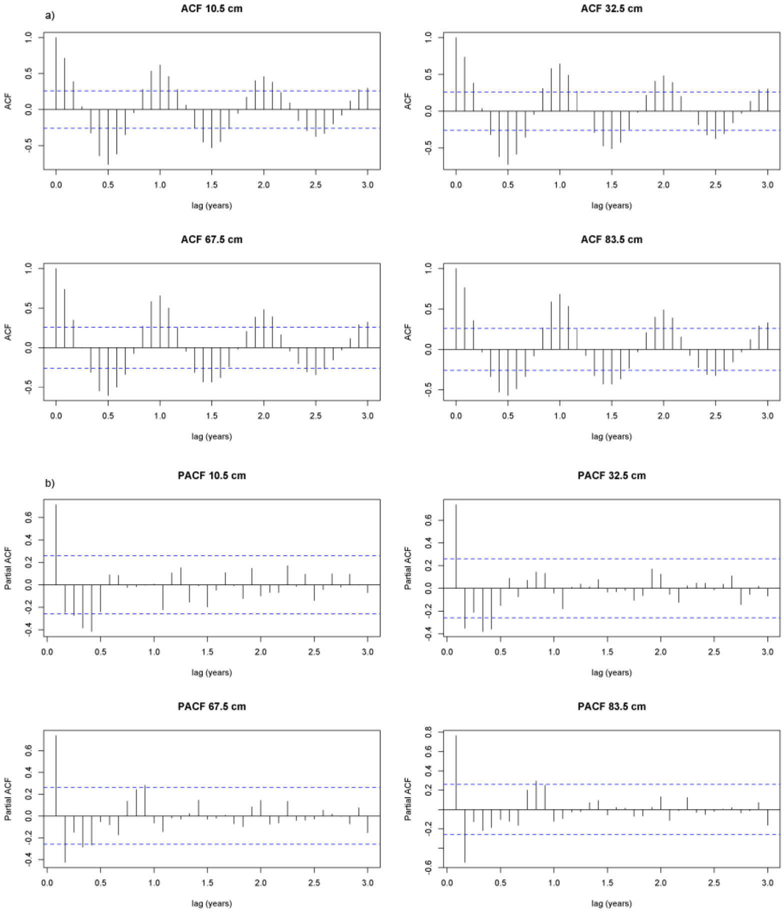

Figure 8. Autocorrelation and partial autocorrelation plots for F1, F2, F3 and F4.

SED
6, 1423–1449, 2014

Active layer thermal monitoring at Fildes Peninsula

R. F. M. Michel et al.

Title Page
Abstract | Introduction
Conclusions | References
Tables | Figures
◂| |▸
◂ ▸
Back | Close
Full Screen / Esc
Printer-friendly Version
Interactive Discussion

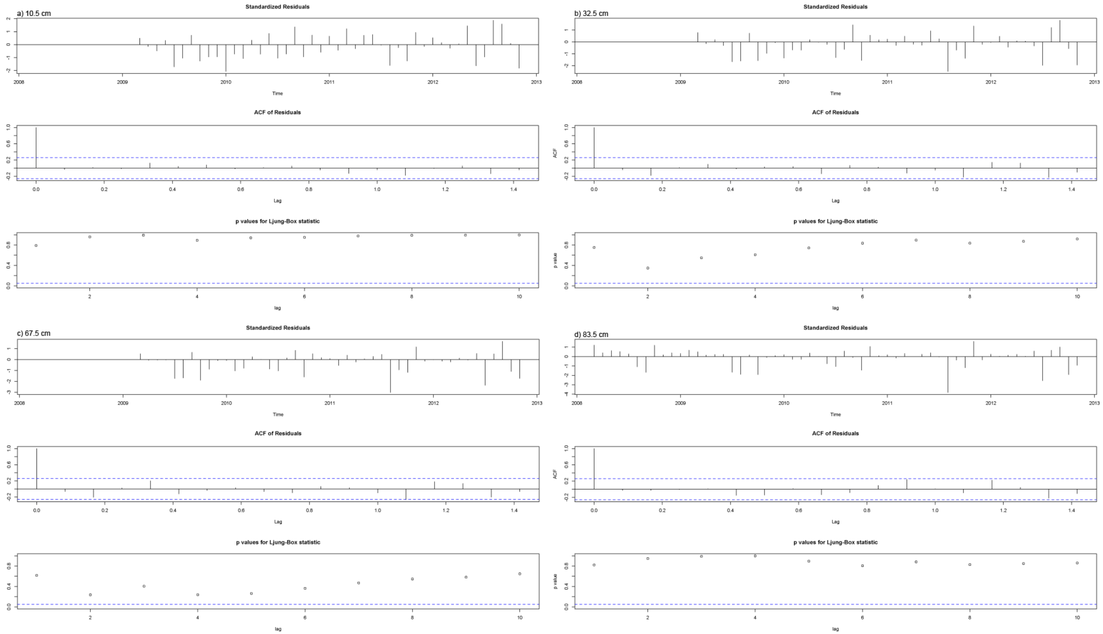

Figure 9. Standardized residuals, autocorrelation plot and Ljung-Box statistics for ARIMA models fitted to F1, F2, F3 and F4.

SED
6, 1423–1449, 2014